Front. Biol. 2010, 5(4): 369–377
DOI 10.1007/s11515-010-0770-6

RESEARCH ARTICLE

The formation of Ca^{2+} gradients at the cleavage furrows during cytokinesis of Zebrafish embryos

Yun-Bo GUO *, Ya WEN *, Wen-Xue GAO *, Jing-Chao LI, Peng ZHOU, Zai-Ling BAI, Bo ZHANG, Shi-Qiang WANG (✉)

State Key Laboratory of Biomembrane and Membrane Biotechnology, and Center of Developmental Biology and Genetics, College of Life Sciences, Peking University, Beijing 100871, China

Abstract In dividing embryos, a localized elevation in intracellular Ca^{2+} ($[Ca^{2+}]_i$) at the cleavage furrow has been shown to be essential for cytokinesis. However, the underlying mechanisms for generating and maintaining these $[Ca^{2+}]_i$ gradients throughout cytokinesis are not fully understood. In the present study, we analyzed the role of inositol 1,4,5-trisphosphate receptors (IP_3Rs) and endoplasmic reticulum (ER) distribution in determining the intracellular Ca^{2+} gradients in early zebrafish blastomeres. Application of the injected Ca^{2+} indicator, Indo-1, showed that during the first cell division a standing Ca^{2+} gradient was formed ~35 min after fertilization, with the $[Ca^{2+}]_i$ spatially decaying from 500–600 nmol/L at the cleavage furrow to 100–200 nmol/L around the nucleus. While the IP_3R immunohistochemical fluorescence was relatively concentrated in the peri-furrow region, ER labeling was relatively enriched in both peri-furrow and peri-nuclear regions. Numeric simulation suggested that a divergence in the spatial distribution of IP_3R and the locations of Ca^{2+} uptake within the ER was essential for the formation of a standing Ca^{2+} gradient, and the Ca^{2+} gradient could only be well-established under an optimal stoichiometry of Ca^{2+} uptake and release. Indeed, while inhibition of IP_3R Ca^{2+} release blocked the generation of the Ca^{2+} gradient at a lower $[Ca^{2+}]_i$ level, both Ca^{2+} release stimulation by inositol 1,4,5-trisphosphate (IP_3) injection and ER Ca^{2+} pump inhibition by cyclopiazonic acid also eliminated the Ca^{2+} gradients at higher $[Ca^{2+}]_i$ levels. Our results suggest a dynamic relationship between ER-mediated Ca^{2+} release and uptake that underlies the maintenance of the peri-furrow Ca^{2+} gradient and is essential for cytokinesis of zebrafish embryos.

Received July 5, 2010; accepted July 23, 2010

E-mail: wsq@pku.edu.cn

*These authors contributed equally to this work

Keywords Ca^{2+} gradients, cytokinesis, zebrafish

1 Introduction

Ca^{2+} is a ubiquitous and versatile messenger in both somatic and germ line cells. Spatiotemporal regulation of Ca^{2+} signals is crucial for many cellular processes, such as mitosis, neuronal activity, exocytosis, and cell proliferation (Krebs and Michalak, 2007). In the early development of eggs and embryos, several distinct Ca^{2+} signals have been discovered, including Ca^{2+} oscillations in the egg after fertilization, Ca^{2+} waves originating from the sperm entry site, and localized Ca^{2+} elevation at the cleavage furrow during cytokinesis (Whitaker, 2006). In 1991, Fluck et al. first discovered in medaka fish eggs that the cytokinesis process is accompanied by slow Ca^{2+} waves moving along the cleavage furrow (Fluck et al., 1991). A similar phenomenon was found in embryos of *Xenopus* and zebrafish (Chang and Meng, 1995; Muto et al., 1996; Webb et al., 1997; Creton et al., 1998; Noguchi and Mabuchi, 2002). Chang and Meng discovered a rapid rise of free Ca^{2+} before furrow initiation in zebrafish embryos, which was gradually developed into Ca^{2+} waves propagating along the forming cleavage furrow, a phenomenon seen also in medaka eggs (Chang and Meng, 1995). The furrow-specific Ca^{2+} increase in zebrafish embryos depends on inositol 1,4,5-trisphosphate receptors (IP_3R)-mediated Ca^{2+} release from internal stores, as blockade of IP_3Rs or chelation of intracellular Ca^{2+} usually leads to failure in cytokinesis (Miller et al., 1993; Chang and Meng, 1995; Webb et al., 1997; Lee et al., 2003). Miller and colleagues showed that the IP_3R-mediated Ca^{2+} release regulates the fusion of vesicles with plasma membrane and the reorganization of contractile band, and is thus necessary for the furrow deepening process (Li et al., 2008).

After fertilization, the Ca^{2+} elevation is usually confined to the peri-furrow region in large eggs, including those of the medaka, zebrafish and frog (Fluck et al., 1991; Chang and Meng, 1995; Muto et al., 1996). This phenomenon contrasts with the Ca^{2+} waves that propagate across the whole egg in many other species, including mammals, echinoderms, fishes, worms and frogs (Gilkey et al., 1978; Hafner et al., 1988; Fontanilla and Nuccitelli, 1998; Deguchi et al., 2000; Samuel et al., 2001). Immunohistochemical study has shown that IP_3Rs are evenly distributed in cortical region in fertilized *Xenopus* eggs (Kume et al., 1993), but not in zebrafish embryos (Lee et al., 2003). These data support the hypothesis that the peri-furrow Ca^{2+} elevation may be attributable to enriched IP_3R in this region. However, this hypothesis does not fully explain why the localized peri-furrow Ca^{2+} elevation lasts for a significant period of time without spreading across the rest of the cell.

In the present work, we quantified the spatial distribution of the intracellular Ca^{2+} concentration ($[Ca^{2+}]_i$), IP_3R expression and endoplasmic reticulum (ER) during early cytokinesis of zebrafish embryos. Our data suggested that a divergent distribution of IP_3R expression and ER network is a key mechanism underlying the formation of a localized, standing intracellular Ca^{2+} gradient, which is required for cytokinesis of the large embryonic blastomeres during the Cleavage Period of zebrafish development.

2 Materials and methods

2.1 Collection of eggs and microinjection

Zebrafishes (*Danio rerio*) were kept in the fish facility of Peking University, Beijing, at 28.5°C with a light/dark cycle of 14 h/10 h. The eggs were collected immediately after spawning and washed several times before being transferred to an embryo medium containing (mmol/L): NaCl 13.7, KCl 0.54, Na_2HPO_4 0.025, KH_2PO_4 0.044, $CaCl_2$ 1.3, $MgSO_4$ 1.0, and $NaHCO_3$ 4.2, at pH 7.2. An agar slab with grooves was used to hold the embryos for injection. We used the Ca^{2+} sensitive fluorescent dyes Indo-1 and Fluo-4 to monitor $[Ca^{2+}]_i$ dynamics in zebrafish embryos. A solution containing 25 mmol/L Indo-1 or Fluo-4 penta potassium salt (Molecular Probes) was injected into the eggs by pressurized air under a dissecting microscope. The volume of injected solution was typically 1% of the egg volume. When inhibitors were used in several experiments, they were mixed with the dyes in the injection solution to monitor the injectate spread. In all experiments, the eggs were injected at the center of the yolk at one-cell stage.

2.2 Determination of free Ca^{2+} concentration

We used the dual-emission Ca^{2+} indicator Indo-1 to determine the free Ca^{2+} concentration and the dynamic range of $[Ca^{2+}]_i$ changes accompanying the cleavage furrow. Embryos injected with Indo-1 penta potassium salt (Molecular Probes) were placed on an inverted fluorescence microscope (Nikon, Japan), and ultraviolet light was used to excite the dye. The emitted light was split at 405 nm and 485 nm with an optical splitter (Cairn Research Ltd., UK) and recorded with a Luca EMCCD camera (Andor Technology, UK). The fluorescence ratio ($R = F_{405}/F_{485}$) was used to calculate the free Ca^{2+} concentration as described by the following equation:

$$[Ca^{2+}] = \beta \cdot K_d \cdot (R - R_{min})/(R_{max} - R)$$

where R is the ratio of fluorescence detected at 405 nm *versus* that detected at 485 nm, R_{min} is the R value when all dyes are free and R_{max} is the R value when all dyes are saturated with Ca^{2+}. β is the ratio of fluorescence at 485 nm in Ca^{2+}-free solution *versus* that in Ca^{2+}-saturated solution. K_d is the dissociation constant of Indo-1. To determine the values of ($\beta \cdot K_d$), R_{min} and R_{max} in the intracellular environment, we used an *in situ* calibration protocol. Briefly, the embryos were injected with ethylene glycol bis (2-aminoethyl ether)-N,N,N',N'-tetraacetic acid (EGTA)-buffered standard Indo-1 potassium salt solutions containing different concentrations of free Ca^{2+}, and the R value was plotted against free Ca^{2+} concentration. The standard curve was then fitted to the equation described above, and values read off the curve are as follows: $R_{max} = 3.8$, $R_{min} = 1.1$ and ($\beta \cdot K_d$) = 2310 nmol/L.

2.3 Labelling IP_3Rs and ER

Immunohistochemical experiments were performed following the protocol described by Lee et al. with slight modification (Lee et al., 2003). Briefly, the paraformaldehyde-fixed dechorionated embryos were washed with phosphate buffer solution (PBS) for more than 5 times to remove excess fixative. The embryos were then washed four times for 5 min each with PBS containing 0.1% Tween-20 (PBT), and then for 5 min with PBT containing 1% dimethylsulfoxide (DMSO) (PBDT). The embryos became very fragile and required careful handling. After incubation for 2 h with a blocking buffer containing 10% bovine serum albumin in PBDT, the embryos were incubated for one hour at room temperature with anti-IP_3R antibody (Type I, Sigma) diluted 1∶500 in blocking buffer. After extensive washes, the embryos were incubated for one hour at room temperature in Cy3-conjugated goat anti-rabbit IgG (Jackson ImmunoResearch Laboratories) diluted 1∶200 in blocking buffer. Then the embryos were washed and prepared for imaging. An ER-specific hydrophobic dye, DiIC18(3) (Molecular Probes), was used to label the ER network in live cells (Terasaki and Jaffe, 1991). A droplet of soybean oil saturated with DiIC18(3) was injected into the yolk at one-cell stage. To allow the dye to diffuse through the entire ER membrane,

observations were made 60–80 min after the injection, when the embryo had divided into 4 cells or 8 cells.

2.4 Confocal microscopy

A Carl Zeiss LSM 510 confocal microscope was used for imaging of dye fluorescence in live cells or Cy3 fluorescence in immunostained embryos. The embryos were immobilized with 1% methylcellulose, and either a top view or a side view was chosen in different experiments. Typically, we used a Plan-Neofluar 10/0.3 objective for Fluo-4/Texas Red imaging and an LD-Achroplan 20/0.4 objective for DiIC18(3) or Cy3 imaging. For Fluo-4/Texas Red imaging, the dyes were excited at 488 nm (Fluo-4) and 543 nm (Texas Red) sequentially, and the emitted fluorescence was band-pass-filtered at 500–550 nm when excited at 488 nm for Fluo-4 imaging, and long-pass-filtered at >560 nm when excited at 543 nm for Texas Red imaging. For DiIC18(3) or Cy3 imaging, the dyes were excited at 543 nm and the fluorescence was long-pass-filtered at >560 nm.

2.5 Simulation

The simulation was based on a one-dimensional space where Ca^{2+} concentration changed according to the following formula:

$$\frac{d[\mathrm{Ca}]_{\mathrm{cytosol}}}{dt} = D_{Ca}\nabla[\mathrm{Ca}]_{\mathrm{cytosol}} + (J_{\mathrm{channel}}\cdot I + J_{\mathrm{pump}}\cdot P) \times (1-b_{\mathrm{cytosol}})$$

$$\frac{d[\mathrm{Ca}]_{\mathrm{ER}}}{dt} = D_{Ca}\nabla[\mathrm{Ca}]_{\mathrm{ER}} - (J_{\mathrm{channel}}\cdot I + J_{\mathrm{pump}}\cdot P)\cdot r$$

where $[Ca]_{cytosol}$ refers to the cytosolic Ca^{2+} concentration; $[Ca]_{ER}$ refers to Ca^{2+} concentration in the ER; D_{Ca} is the diffusion coefficient for Ca^{2+}; I is distribution of IP_3Rs and given by function $I(x)= 1-x/(2a)$, in which a is the number of spatial units in the model; P is distribution of Ca^{2+} pumps and given by function $P(x)=(2x/a-1)^2/5+0.8$; The b value defines the capacity of Ca^{2+} buffers in the cytosol, given by the percentage of total Ca^{2+} occupied by buffers. The r value defines the volume ratio of cytosol *versus* ER; $J_{channel}$ and J_{pump} are Ca^{2+} fluxes through IP_3Rs and Ca^{2+} pumps respectively, which were given as follows:

$$J_{\mathrm{channel}} = V_{\max}^{\mathrm{channel}}([\mathrm{Ca}]_{\mathrm{ER}} - [\mathrm{Ca}]_{\mathrm{cytosol}})$$

$$J_{\mathrm{pump}} = \frac{V_{\max}^{\mathrm{pump}}}{1+\left(K_{\mathrm{pump}}/([\mathrm{Ca}]_{\mathrm{cytosol}} - [\mathrm{Ca}]_{\min})\right)^{h}}$$

in which V_{max} refers to maximal Ca^{2+} transport of the channel or the pump; $[Ca]_{min}$ refers to the minimal Ca^{2+} concentration required for the Ca^{2+} pump to function; h is the Hill coefficient; and K_{pump} is the Michaelis-Menten constant of Ca^{2+}- dependent pump activity (See Table 1 for the values of parameters used in the simulation).

2.6 Statistics

Data were presented as mean±SE. Student's *t*-test or two way analysis of variance with repeated measures was used to determine the significance of differences.

3 Results

3.1 Measurement of $[Ca^{2+}]_i$ gradient before and during furrow formation

In order to determine the spatial distribution and temporal development of $[Ca^{2+}]_i$, we injected the Ca^{2+}-indicator, Indo-1, into the zebrafish eggs after fertilization. At the concentration we used, the injection of dyes did not interfere with the normal cytokinesis process of the embryos: the cleavage furrow invagination occurred normally at the top of animal pole 30–35 min after fertilization (Fig. 1A), and a deep furrow was formed separating two daughter cells in an additional 10–15 min. To determine the absolute $[Ca^{2+}]_i$, we calculated the ratio (R) of the Indo-1 fluorescence emitted at 405 nm *versus* that at 485 nm increased at the furrow. The dual wavelength emission feature of Indo-1 allows a dye

Table 1 Parameters used in the simulation

parameters	meaning	value
D_{Ca}	diffusion coefficient of Ca^{2+}	100 μm^2/s
b	percentage of cytosolic Ca^{2+} occupied by Ca^{2+} buffers	93%
r	volume ratio of cytosol *versus* ER	25
$V_{\max}^{\mathrm{channel}}$	maximal transport speed of IP_3R	0.02/s
$V_{\max}^{\mathrm{pump}}$	maximal transport speed of Ca^{2+} pump	15 μmol Ca^{2+}/L cytosol·s^{-1}
K_{pump}	Michaelis-Menten coefficient of Ca^{2+}-dependent Ca^{2+} pump activity	0.18 μmol/L
h	Hill coefficient of Ca^{2+} binding to the pump	3.9
$[Ca]_{min}$	minimal Ca^{2+} concentration required for the pump to function	50 μmol/L

concentration-independent ratiometric quantification of $[Ca^{2+}]_i$, so that the absolute $[Ca^{2+}]_i$ could be determined. We found that the localized $[Ca^{2+}]_i$ increase started at 25–30 min after fertilization (Fig. 1A, left), even before the initiation of the membrane invagination. When the $[Ca^{2+}]_i$ developed to and was maintained at ~370 nmol/L (Fig. 1B, red curve), the furrow appeared, elongated and deepened. This elevation of $[Ca^{2+}]_i$ appeared as a standing Ca^{2+} gradient, as a region ~100 μm away from the furrow only exhibited a slight increase in $[Ca^{2+}]_i$ (Fig. 1B, blue curve). Measurement of $[Ca^{2+}]_i$ at different locations showed that there was a standing Ca^{2+} gradient spatially decaying from 500–600 nmol/L at the cleavage furrow to 100–200 nmol/L around the nucleus (Fig. 1C).

Earlier reports using calcium green-1 or aequorin as Ca^{2+} probes (Chang and Meng, 1995; Webb et al., 1997; Creton et al., 1998) have shown that local Ca^{2+} increase occurs at the cleavage furrow and is maintained throughout the process of furrow development. Our results showed that localized increases in $[Ca^{2+}]_i$ resulted in the formation of a transient standing Ca^{2+} gradient between regions of the blastomere participating in the process of cytokinesis and those that did not. Our new data derived from the use of a dual wavelength fluorescent Ca^{2+} reporter (i.e., Indo-1) thus confirm and support previous reports using single wavelength fluorescent Ca^{2+} reporters, i.e., Ca^{2+} Green-dextran (Chang and Meng, 1995) and luminescent Ca^{2+} reporters, i.e., aequorin (Fluck et al., 1991; Webb et al., 1997; Creton et al., 1998).

3.2 Divergence of the intracellular distribution of IP_3Rs and ER

The early development of zebrafish was not affected when the extracellular medium was replaced with Ca^{2+}-free solution, but was blocked by inhibiting IP_3R-mediated Ca^{2+} release from ER (Chang and Meng, 1995). To investigate the role of intracellular distribution of IP_3Rs and ER Ca^{2+} stores in the spatial gradient of $[Ca^{2+}]_i$, we performed immunohistochemical staining of IP_3Rs. We found that the IP_3Rs were moderately enriched at the cleavage furrow (Fig. 2A, arrows), exhibiting a decaying IP_3R density from the furrow region to the peri-nucleus region (Fig. 2C, blue curve).

By contrast, labeling of ER in live embryos with the ER-specific fluorescent dye DiIC18(3) showed that the ER distributed throughout the intracellular space, with a moderate enrichment in both the furrow (Fig. 2B, arrows) and the peri-nucleus (Fig. 2B, arrowhead) areas (Fig. 2C, red curve).

We hypothesized that the divergent patterns of IP_3R and ER distributions might play an important role in generating

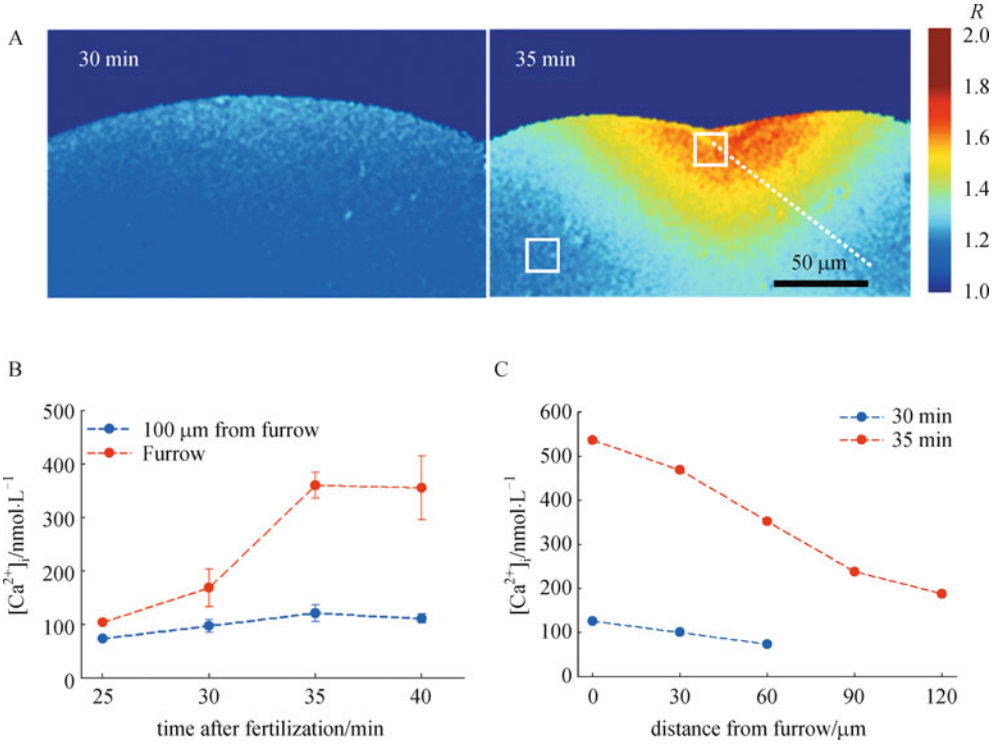

Fig. 1 Ca^{2+} elevation at the furrow revealed by Indo-1. A: The Indo-1 fluorescence ratio R (F_{405}/F_{485}) increased gradually at the top of the animal pole. The squares denote sample regions at the furrow and 100 μm away from it. The dashed line indicates the sampling direction used to measure Ca^{2+} gradient in panel C. The scale bar represents 50 μm. B: Free Ca^{2+} level at the furrow increased as the furrow initiated and developed, while the sample region 100 μm away remained at the resting Ca^{2+} level. C: Ca^{2+} gradient growing in 30 (blue) ~35 (red) min after fertilization.

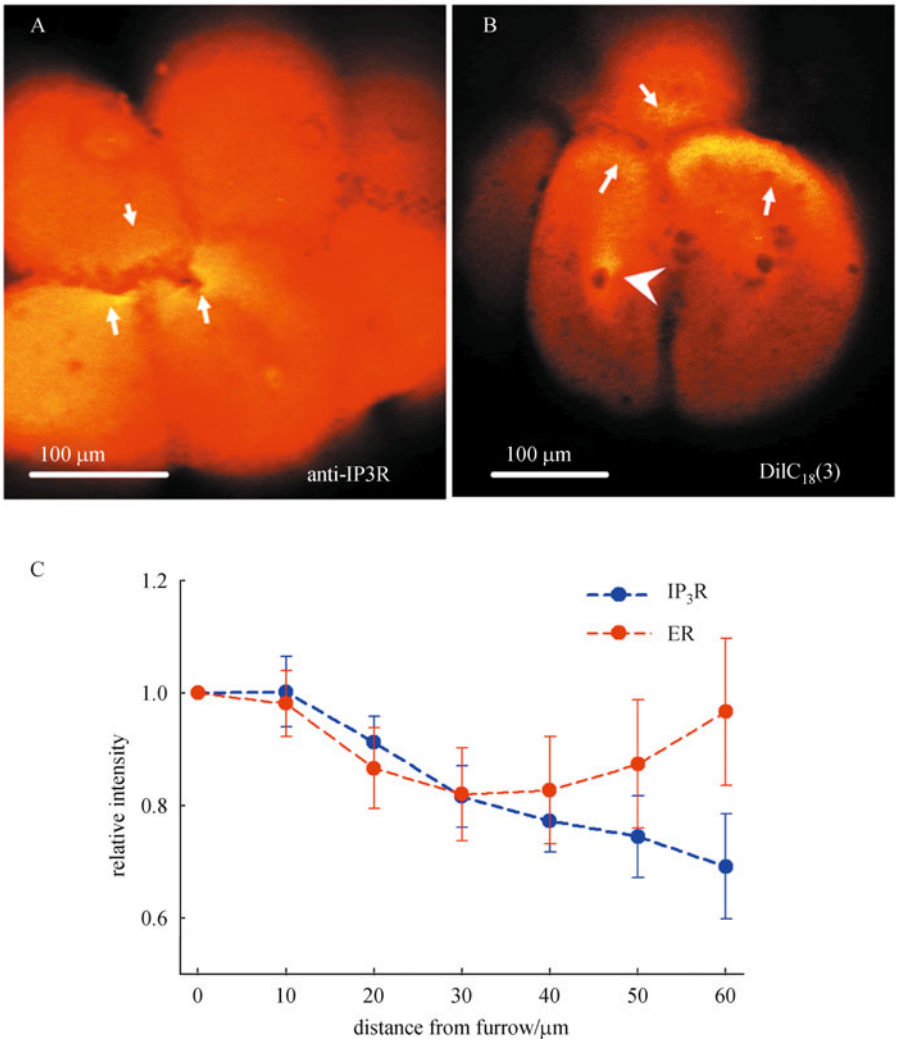

Fig. 2 Distribution of IP_3Rs and ER in cleaving zebrafish embryos. A: Immunostaining using the antibody against type 1 IP_3R (Anti-IP_3R1) revealed moderate enrichment of IP_3Rs at the furrow region. Arrows denote the areas with enrichment. B: The ER-specific dye, DilC18(3), is enriched both at the furrow and around the nucleus. Arrows denote enrichment of ER near the furrow, while the arrowhead denotes enrichment of ER near the nucleus. Scale bars in both panels represent 100 μm. C: Relative intensities of IP_3Rs and ER. The fluorescence intensity of immunostaining or ER dye along a line selected from the furrow to the nucleus was normalized to the value at the furrow. Data were averaged from at least 3 embryos for each labeling.

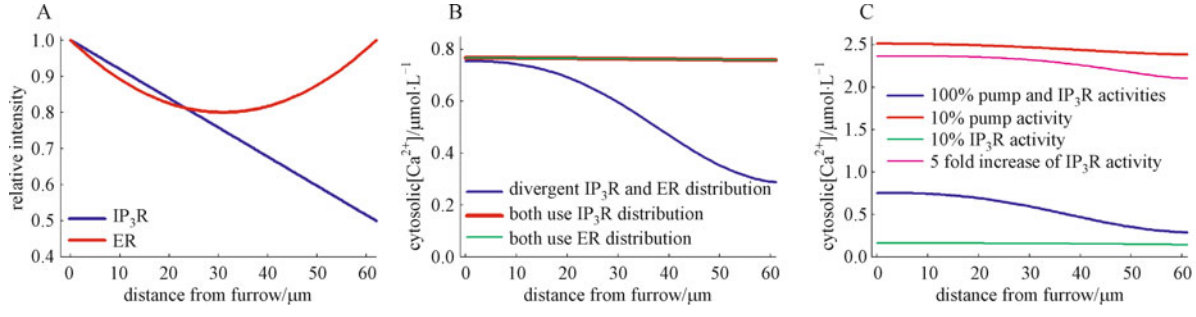

Fig. 3 Simulation of Ca^{2+} gradient. A: Linear and parabolic distributions were used for IP_3R and ER, respectively, in the simulation. We assume that the Ca^{2+} pumps are evenly distributed in the ER. B: Simulated Ca^{2+} concentration from the furrow to the nucleus. With divergent IP_3Rs and ER distributions shown in A, the Ca^{2+} gradient was formed (blue), while the same ER and IP_3R distribution gave nearly homogenous Ca^{2+} concentration (red, green). C: Effects of altering IP_3R and Ca^{2+} pump activities on Ca^{2+} gradient. Decreasing V_{max} of IP_3R (see **Methods**) to 10% could keep Ca^{2+} concentration at resting level (green), while decreasing V_{max} of Ca^{2+} pump to 10% caused homogeneous increase of Ca^{2+} concentration and eliminated the Ca^{2+} gradient (red). Increasing V_{max} of IP_3R by 5 fold also caused homogeneous Ca^{2+} elevation and damped Ca^{2+} gradient (pink).

the standing Ca^{2+} gradient in dividing embryos. As a proof-of-principle, we built a simplified model to simulate the Ca^{2+} dynamics in zebrafish embryos. Because ER Ca^{2+} pump distribution could not be measured due to the lack of antibody that works in fish, we assumed for the sake of the model that Ca^{2+} pumps distributed evenly on the ER membrane. Based on experimental results (Fig. 2C), we used a linear curve for IP_3R distribution and a parabolic curve for ER Ca^{2+} pump distribution (Fig. 3A). With proper parameters set for Ca^{2+} pools, Ca^{2+} cycling kinetics and Ca^{2+} buffers, the divergent IP_3R/Ca^{2+} pump distribution resulted in a standing Ca^{2+} gradient (Fig. 3B, blue), which well reproduced the decaying $[Ca^{2+}]_i$ from the furrow in experimental data (Fig. 1C). When we used identical distribution pattern (either linear or parabolic) for both IP_3Rs and Ca^{2+} pumps, the Ca^{2+} gradient was abolished (Fig. 3B, red and green), no matter which distribution pattern was used for simulation. This result suggested that the divergence of IP_3R and Ca^{2+} pump distribution may be important in the generation of the standing Ca^{2+} gradient during early zebrafish cytokinesis.

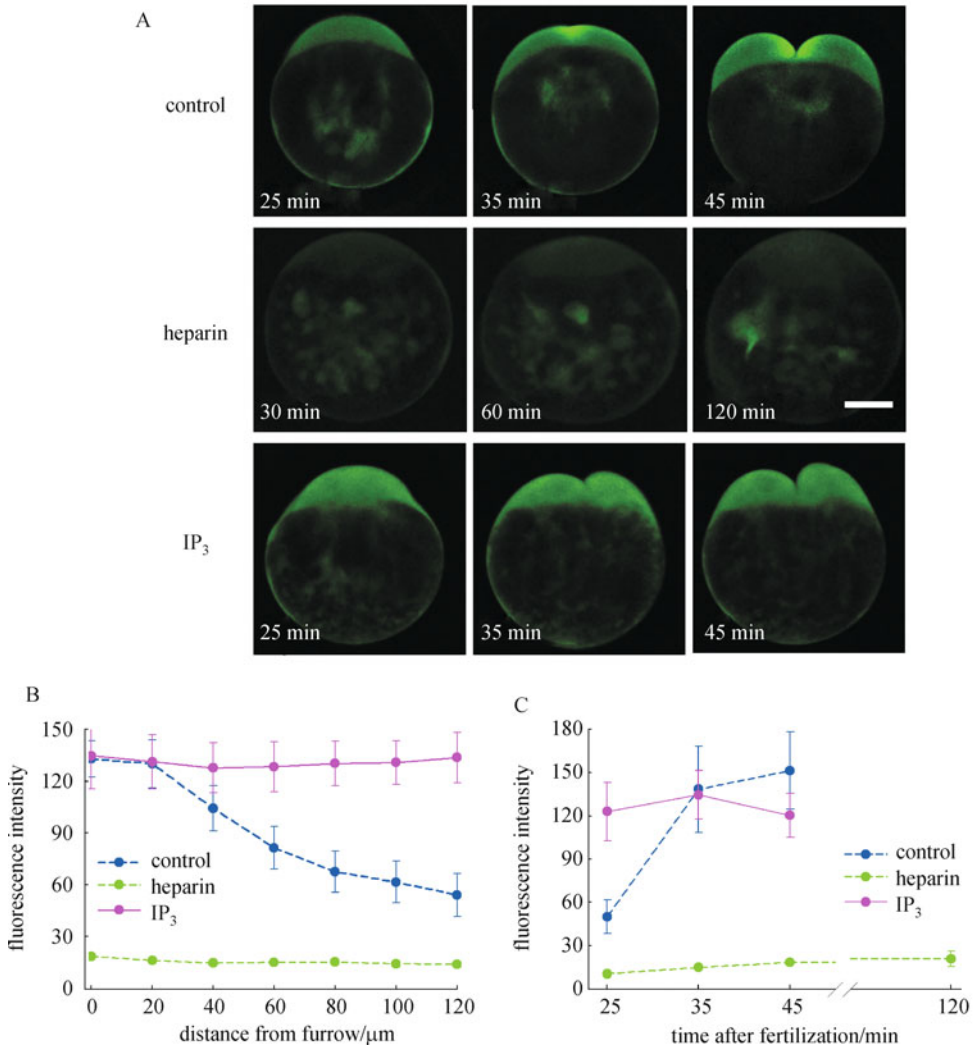

Fig. 4 Injection of heparin blocked Ca^{2+} elevation and furrow initiation. Embryos were injected with Fluo-4 to indicate the Ca^{2+} concentration. A: Top: In control embryos, the furrow formed between 35 and 45 min after fertilization, which was accompanied by the local Ca^{2+} elevation. Middle: Ca^{2+} elevation was blocked in embryos injected with 0.1 mg/mL heparin. The furrow failed to form, and the morphology of the blastoderm remained unchanged for at least 2 h after fertilization. Bottom: Injection of 10 μmol/L IP_3 elevated Ca^{2+} concentration homogeneously in the blastoderm, but did not affect the furrow formation. Scale bar represents 200 μm and applies to all panels. B: Effects of heparin and IP_3 treatments on Ca^{2+} gradient. Heparin prevented Ca^{2+} elevation (green), while IP_3 induced homogeneous Ca^{2+} elevation (pink), and both treatments abolished the Ca^{2+} gradient. 3–5 embryos were sampled for each group. C: Fluo-4 fluorescence intensity in furrow area (and putative furrow area in the case of heparin-injected embryos). Data collected from the same embryos in B. Control embryos showed a marked increase of Fluo-4 fluorescence as furrow progressed (blue), and IP_3 induced early Ca^{2+} elevation by directly activating IP_3Rs (pink), while in heparin treated embryos, the fluorescence remained low even 2 h after fertilization (green).

3.3 Importance of the coordination of Ca^{2+} transporters

Intracellular Ca^{2+} homeostasis is maintained by a delicate cooperation between Ca^{2+} channels and transporters. In order to explore whether and how the cooperation of IP_3R Ca^{2+} release and ER Ca^{2+} uptake influences the Ca^{2+} gradient formation, we modulated the strength of IP_3R Ca^{2+} release and Ca^{2+} pumps in the simulation model. When the Ca^{2+} fluxes through IP_3Rs were reduced to 10%, the $[Ca^{2+}]_i$ was kept at a much lower level, and the Ca^{2+} gradient could not be developed (Fig. 3C, green). Reversely, When the Ca^{2+} fluxes through IP_3Rs were increased by 5-fold, although the $[Ca^{2+}]_i$ reached a much higher level, the Ca^{2+} gradient was significantly compromised (Fig. 3C, pink). Similarly, when we reduced the Ca^{2+} pump activity to 10%, the $[Ca^{2+}]_i$ also increased globally to a much higher level without forming a Ca^{2+} gradient (Fig. 3C, red). These simulations suggested that a precise coordination between IP_3R-mediated Ca^{2+} release and ER Ca^{2+} uptake was critical for the generation of a standing Ca^{2+} gradient.

We then validated the simulation by experiments. To monitor the $[Ca^{2+}]_i$, fertilized oocytes were injected with fluorescent Ca^{2+} indicator Fluo-4, which did not interfere with the normal formation of furrow and Ca^{2+} gradient (Fig. 4A, upper panels; Figs. 4B and C, blue lines). When the oocytes were injected with the IP_3R inhibitor heparin (0.1 mg/mL), the $[Ca^{2+}]_i$, as represented by Fluo-4 fluorescence, remained low without forming a Ca^{2+} gradient (Fig. 4A, middle panels; Figs. 4B and C, green). Reversely, stimulating IP_3R activity with 10 μmol/L IP_3 caused global elevation of intracellular Ca^{2+} (Fig. 4A, lower panels; Fig. 4C, pink line), eliminating the Ca^{2+} gradient (Fig. 4B, pink). Similar to IP_3 treatment, inhibiting Ca^{2+} pump with 10 μmol/L cyclopiazonic acid (CPA) also caused homogenous Ca^{2+} elevation (Figs. 5A and C, red) and abolished the Ca^{2+} gradient (Fig. 5B).

Both experimental and model simulation suggest that a degree of coordination between the IP_3R-mediated Ca^{2+} release and ER Ca^{2+} uptake is a key requirement for the Ca^{2+} gradient formed during cytokinesis. There is likely to

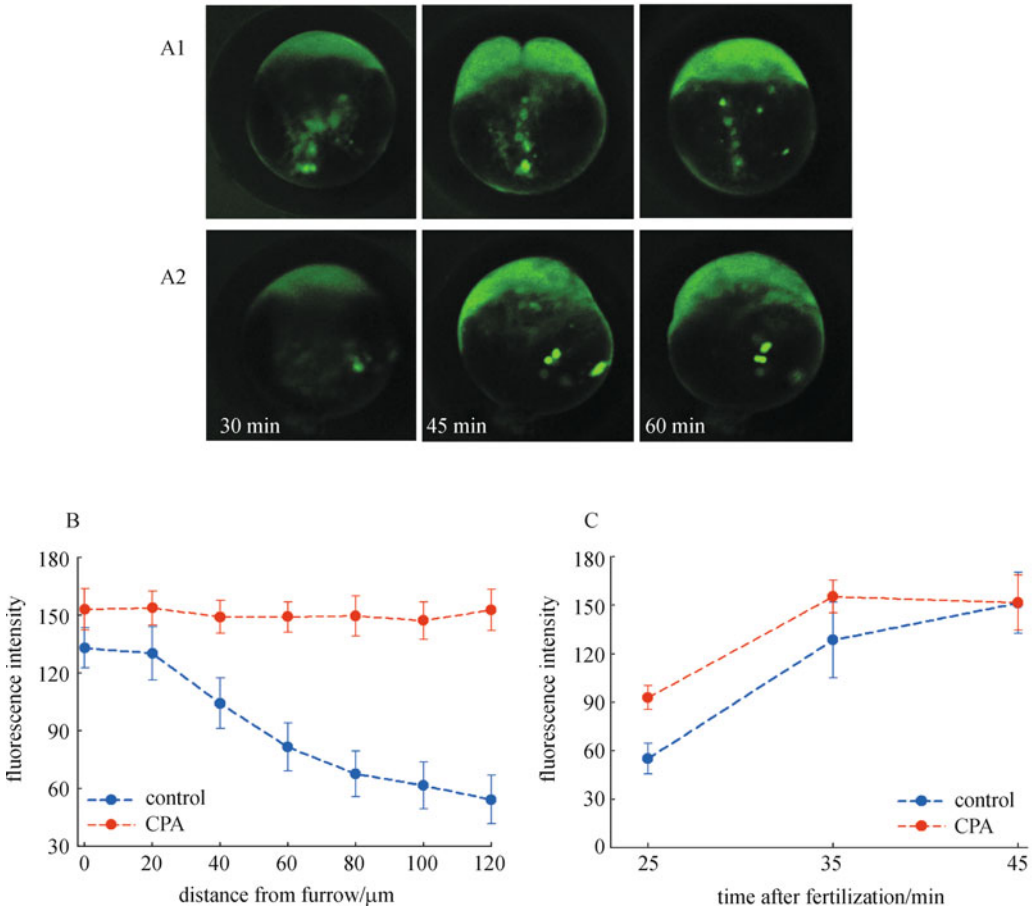

Fig. 5 Homogenous Ca^{2+} elevation perturbed the furrow formation. Inhibition of ER Ca^{2+} pump with 10 μmol/L cyclopiazonic acid (CPA) caused homogenous Ca^{2+} elevation in the blastoderm. The furrow either could not form (A2), or regressed soon after its formation (A1). Scale bar represents 200 μm and applies to all panels. B: The CPA-treated embryos lost the Ca^{2+} gradient. Data were from at least 3 embryos for each group. C: Fluo-4 fluorescence in furrow area. Like IP_3 treatment, CPA also caused earlier Ca^{2+} elevation (25 min). Data were from same embryos in B.

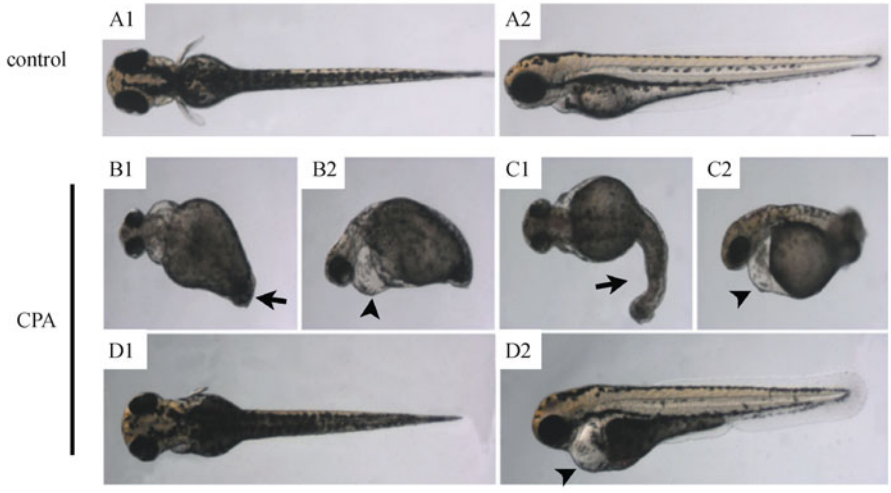

Fig. 6 CPA treatment induced malformation of tails and pericardial edema. A: Untreated embryo. B–D: Embryos were incubated with 100 μmol/L CPA at different developmental stages and imaged 72 h after fertilization. Arrows and arrowheads denote tail defects and pericardial edemas, respectively. B: Embryos treated at segmentation period. C: Embryos treated at pharyngula period. D: Embryos treated at hatching period. Scale bars = 200 μm. Left (A1–D1): dorsal view; Right (A2–D2): lateral view of the corresponding embryos in A1–D1.

be, however, a complex interaction between IP_3R distribution, IP_3R sensitivity, and the various up-stream elements in the phosphatidylinositol (PI) signaling pathway that may play a role in the signaling cascades involved in modulating localized domains of $[Ca^{2+}]_i$ during cytokinesis. For example, it has been reported in other cell types that phosphotidylinositol 4,5-biphosphate (PIP2), the precursor of inositol 1,4,5-triphosphate (IP_3), and phospholipase C that catalyzes PIP2 into IP_3 are localized to the cleavage furrow during cytokinesis (Wong et al., 2005; Naito et al., 2006). It remains to be tested whether the IP_3-generating process is also quantitatively important in the Ca^{2+} gradient formation in zebrafish embryos.

4 Discussion

Classic studies using BAPTA-type Ca^{2+} buffers demonstrated that Ca^{2+} elevation in embryos is essential for the completion of cytokinesis, and a facilitated diffusion theory was proposed to explain the higher efficacy of Ca^{2+} buffers with medium K_d values to block cytokinesis of vertebrate embryos (Speksnijder et al., 1989; Miller et al., 1993; Snow and Nuccitelli, 1993). This hypothesis highlights the importance of localized $[Ca^{2+}]_i$ in the completion of cytokinesis (Miller et al., 1993).

In our experiments, injection of IP_3 to directly activate IP_3Rs or CPA to inhibit the ER Ca^{2+} pumps caused a homogeneous Ca^{2+} elevation in the blastomeres (Figs. 4 and 5), thus eliminating any Ca^{2+} gradients. We found that disrupting Ca^{2+} gradient formation caused developmental defects. The heparin-injected embryos failed to form the cleavage furrow 2 h after fertilization (Fig. 4A, middle panels). Although most CPA-treated embryos developed normally into blastula stage, some embryos did exhibit failure or regression of cleavage furrows (Fig. 5A). Moreover, incubation of the embryos in later stages with CPA-containing medium caused a variety of morphological defects. For example, transient treatment of embryos with 100 μmol/L CPA at segmentation, pharyngula or hatching periods resulted in pericardial edemas (Figs. 6B–D, arrowheads). CPA treatment in segmentation or pharyngula period led to abnormal tail development (Figs. 6B and C, arrows). As CPA does not prevent the elevation of intracellular Ca^{2+}, the developmental effect of CPA suggested that not only the elevation of Ca^{2+} concentration but also the precise coordination of Ca^{2+} transporters in generating an appropriate Ca^{2+} gradient are important in embryo development.

To summarize, in the present study, we quantified the intracellular Ca^{2+} gradient during early cell divisions in zebrafish embryos, and we propose that the divergence of IP_3R and ER Ca^{2+} pump distribution contributes to the formation of localized, standing Ca^{2+} gradients, which are crucial for the successful completion of cytokinesis.

Acknowledgements This study was supported by the National Natural Science Foundation of China (Nos. 30730013, 30721064, and 30728012). We would like to thank Ling WEI, Yan-Ting ZHAO and Hao-Di WU for critical reading of the manuscript.

References

Chang D C, Meng C (1995). A localized elevation of cytosolic free calcium is associated with cytokinesis in the zebrafish embryo. J Cell Biol, 131(6 Pt 1): 1539–1545

Créton R, Speksnijder J E, Jaffe L F (1998). Patterns of free calcium in

zebrafish embryos. J Cell Sci, 111(Pt 12): 1613–1622

Deguchi R, Shirakawa H, Oda S, Mohri T, Miyazaki S (2000). Spatiotemporal analysis of Ca(2 +) waves in relation to the sperm entry site and animal-vegetal axis during Ca(2 +) oscillations in fertilized mouse eggs. Dev Biol, 218(2): 299–313

Fluck R A, Miller A L, Jaffe L F (1991). Slow calcium waves accompany cytokinesis in medaka fish eggs. J Cell Biol, 115(5): 1259–1265

Fontanilla R A, Nuccitelli R (1998). Characterization of the sperm-induced calcium wave in Xenopus eggs using confocal microscopy. Biophys J, 75(4): 2079–2087

Gilkey J C, Jaffe L F, Ridgway E B, Reynolds G T (1978). A free calcium wave traverses the activating egg of the medaka, Oryzias latipes. J Cell Biol, 76(2): 448–466

Hafner M, Petzelt C, Nobiling R, Pawley J B, Kramp D, Schatten G (1988). Wave of free calcium at fertilization in the sea urchin egg visualized with fura-2. Cell Motil Cytoskeleton, 9(3): 271–277

Krebs J, Michalak M (2007). Calcium: A Matter of Life or Death. Amsterdam: Elsevier B.V.

Kume S, Muto A, Aruga J, Nakagawa T, Michikawa T, Furuichi T, Nakade S, Okano H, Mikoshiba K (1993). The Xenopus IP3 receptor: structure, function, and localization in oocytes and eggs. Cell, 73(3): 555–570

Lee K W, Webb S E, Miller A L (2003). Ca2+ released via IP3 receptors is required for furrow deepening during cytokinesis in zebrafish embryos. Int J Dev Biol, 47(6): 411–421

Li W M, Webb S E, Chan C M, Miller A L (2008). Multiple roles of the furrow deepening Ca2+ transient during cytokinesis in zebrafish embryos. Dev Biol, 316(2): 228–248

Miller A L, Fluck R A, McLaughlin J A, Jaffe L F (1993). Calcium buffer injections inhibit cytokinesis in Xenopus eggs. J Cell Sci, 106 (Pt 2): 523–534

Muto A, Kume S, Inoue T, Okano H, Mikoshiba K (1996). Calcium waves along the cleavage furrows in cleavage-stage Xenopus embryos and its inhibition by heparin. J Cell Biol, 135(1): 181–190

Naito Y, Okada M, Yagisawa H (2006). Phospholipase C isoforms are localized at the cleavage furrow during cytokinesis. J Biochem, 140 (6): 785–791

Noguchi T, Mabuchi I (2002). Localized calcium signals along the cleavage furrow of the Xenopus egg are not involved in cytokinesis. Mol Biol Cell, 13(4): 1263–1273

Samuel A D, Murthy V N, Hengartner M O (2001). Calcium dynamics during fertilization in C. elegans. BMC Dev Biol, 1: 8–13

Snow P, Nuccitelli R (1993). Calcium buffer injections delay cleavage in Xenopus laevis blastomeres. J Cell Biol, 122(2): 387–394

Speksnijder J E, Miller A L, Weisenseel M H, Chen T H, Jaffe L F (1989). Calcium buffer injections block fucoid egg development by facilitating calcium diffusion. Proc Natl Acad Sci U S A, 86(17): 6607–6611

Terasaki M, Jaffe L A (1991). Organization of the sea urchin egg endoplasmic reticulum and its reorganization at fertilization. J Cell Biol, 114(5): 929–940

Webb S E, Lee K W, Karplus E, Miller A L (1997). Localized calcium transients accompany furrow positioning, propagation, and deepening during the early cleavage period of zebrafish embryos. Dev Biol, 192(1): 78–92

Whitaker M (2006). Calcium at fertilization and in early development. Physiol Rev, 86(1): 25–88

Wong R, Hadjiyanni I, Wei H C, Polevoy G, McBride R, Sem K P, Brill J A (2005). PIP2 hydrolysis and calcium release are required for cytokinesis in Drosophila spermatocytes. Curr Biol, 15(15): 1401–1406